CHAPTER

Fluorescent Protein Applications in Microscopy

5

Whitney L. Johnson and Aaron F. Straight

Department of Biochemistry, Stanford Medical School, Stanford University, Stanford, California, USA

CHAPTER OUTLINE

Abstract

The use of fluorescent proteins (FPs) in modern cell biology and microscopy has had an extraordinary impact on our ability to investigate dynamic processes in living cells. FPs are unique in that fluorescence is encoded solely by the primary amino

Methods in Cell Biology, Volume 114 **ISSN 0091-679X**

http://dx.doi.org/10.1016/B978-0-12-407761-4.00005-1

acid sequence of the FP and does not require enzymatic modification or cofactors. This genetically encoded fluorescence enables the expression of FPs in diverse cells and organisms and the detection of that fluorescence in living systems. This chapter focuses on microscopy-based applications of FP detection to monitor protein localization, dynamics, interaction, and the cellular environment.

5.1 THE IDENTIFICATION OF GREEN FLUORESCENT PROTEIN

The isolation of green fluorescent protein (GFP) was first described by Shimomura, Johnson, & Saiga, 1962 as a footnote to their studies about the aequorin protein from the jellyfish *Aequorea aequorea*. *A. aequorea* normally emits a greenish luminescence from the light organs around the rim of the jellyfish. During the isolation of the luminescence system of *Aequorea*, Shimomura and colleagues noted that the luminescence from aequorin was blue rather than the green luminescence of the intact organism. However, they also noted that

> *A protein giving solutions that look slightly greenish in sunlight though only yellowish under tungsten lights, and exhibiting a very bright, greenish fluorescence in the ultraviolet of a Mineralite, has also been isolated from squeezates. No indications of a luminescent reaction of this sustance [sic] could be detected. Studies of the emission spectra of both this protein and aequorin are in progress.*

Shortly after their observation of the green fluorescence, the protein was purified and characterized and eventually given the name green fluorescent protein (Hastings & Morin, 1969; Johnson et al., 1962).

Prior to the cloning of GFP, its fluorescent properties were characterized in detail through careful biochemical analysis. Purified aequorin emits blue light when stimulated with calcium as the result of oxidation of coelenterazine to coelenteramide, but the light organs of *Aequorea* emit a greenish light upon stimulation of the organism. Morin and Hastings provided an explanation for this wavelength shift by demonstrating that the excited state energy of calcium-stimulated aequorin could be transferred to GFP via the Förster mechanism, resulting in the longer wavelength green emission from GFP (Fig. 5.1; Morin & Hastings, 1971). Through a combination of intuition and brute force biochemistry, Shimomura, 1979 first deciphered the structure of the GFP chromophore as a *p*-hydroxybenzyl imidazolone. GFP was even crystallized in 1974 using protein isolated from tens of thousands of jellyfish, and the energy transfer reaction between aequorin and GFP was studied in detail (Morise, Shimomura, Johnson, & Winant, 1974).

Although these elegant biochemical studies had demonstrated many of the properties of GFP, the experiments that catapulted GFP into widespread use were the cloning of the gene for GFP from *Aequorea* and the subsequent expression of the protein in other organisms. Prasher, Eckenrode, Ward, Prendergast, & Cormier, 1992 isolated a full-length cDNA clone encoding GFP, and the primary sequence demonstrated that the chromophore of the protein was derived from the amino acid triplet Ser-Tyr-Gly at positions 65-66-67. Chromophore formation is resulted from cyclization of the peptide backbone and oxidation of the tyrosine side chain (Cody, Prasher, Westler, Prendergast, & Ward, 1993), but as Cody et al. pointed out

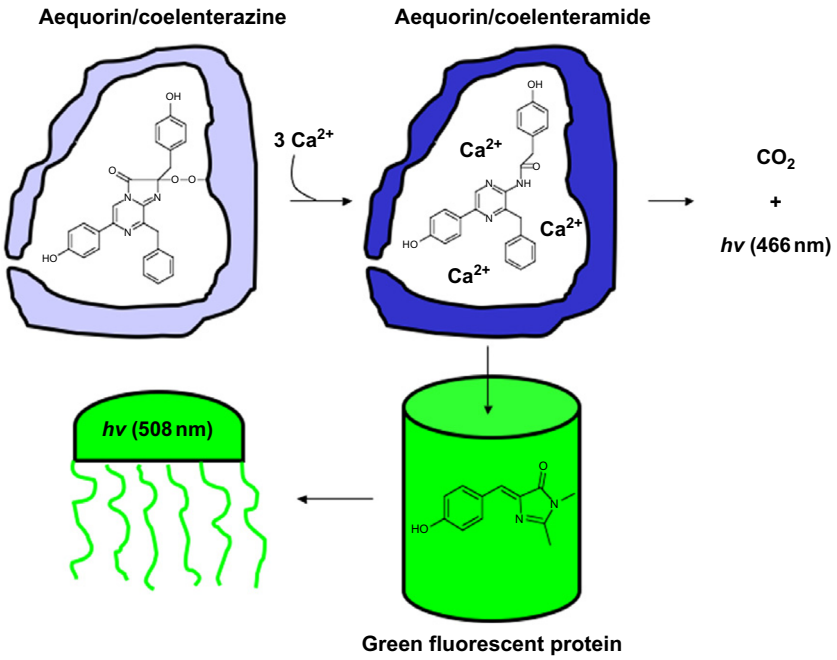

FIGURE 5.1

Energy transfer between aequorin and GFP. Aequorin with its attached cofactor coelenterazine is stimulated to luminesce when calcium ions bind. In the absence of GFP, aequorin emits light of 466 nm. In the presence of GFP, the excited state energy of aequorin can be transferred to GFP resulting in the longer wavelength emission at 508 nm.

> *It is very unlikely that the chromophore forms spontaneously, but its formation probably requires some enzymatic machinery.*

Truly surprising were the experiments that followed from Chalfie, Tu, Euskirchen, Ward, & Prasher, 1994 and Inouye & Tsuji, 1994 showing that GFP could be expressed in other organisms and still become fluorescent. This demonstrated that no *Aequorea* specific cofactors were required for chromophore formation, and also led to the realization that GFP could be used in virtually any organism to track gene expression, protein dynamics, and more. The discovery, characterization, and optimization of GFP have since revolutionized imaging in live biological systems, and earned Osamu Shimomura, Martin Chalfie, and Roger Y. Tsien the Nobel Prize in Chemistry in 2008.

5.2 FORMATION OF THE GFP CHROMOPHORE

The primary amino acid sequence of GFP is sufficient to direct the formation of the functional chromophore. Heim, Prasher & Tsien, 1994 first proposed a reaction scheme to explain how GFP might spontaneously mature into a fluorescent protein

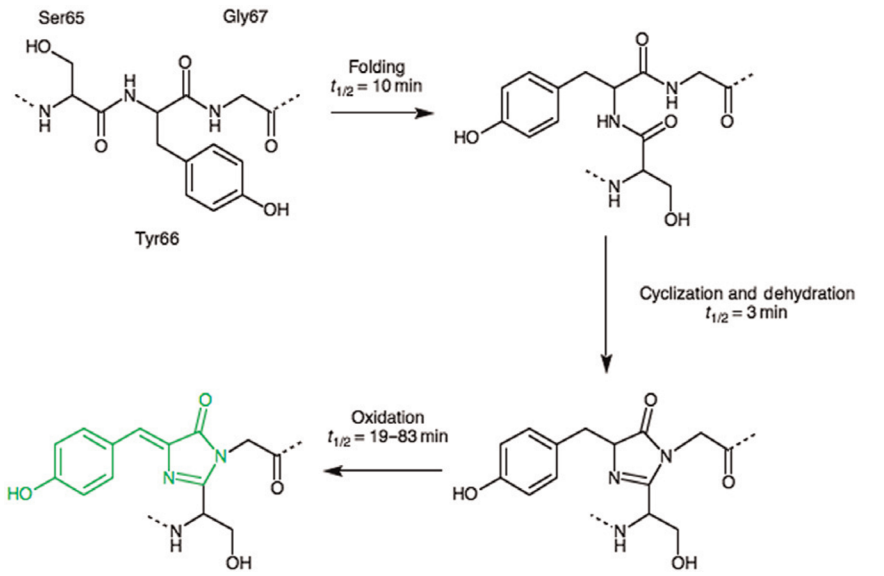

FIGURE 5.2

Formation of the GFP chromophore. Three steps in GFP chromophore formation are shown. The first step is the folding of the GFP protein that has a half-time of approximately 10 min. Once folded, cyclization of the peptide backbone and dehydration occur rapidly. The rate-limiting step in chromophore formation is the oxidation of the tyrosine side chain. The final deprotonation of the tyrosine hydroxyl group is not shown.

(FP; Fig. 5.2). Four key steps were proposed to control chromophore formation: (1) the folding of the GFP protein, (2) the cyclization and dehydration of the peptide backbone between the amide nitrogen of Gly67 and the carbonyl of Ser65, (3) the oxidation of the Tyr66 side chain to introduce a vinyl group, and (4) the deprotonation of the Tyr66 hydroxyl. The rate constants for each step in GFP chromophore formation have been measured, and the rate-limiting step in the reaction is the oxidation of the Tyr66 side chain (Reid & Flynn, 1997).

The initial folding of the GFP molecule precedes all other steps in chromophore formation. As researchers began to express GFP in a variety of organisms, it was quickly realized that the conversion of GFP to its fluorescent state was highly temperature dependent. Expression of GFP at 37 °C in *Escherichia coli* resulted in most of the protein being incorporated into inclusion bodies, while expression at 25 °C produced soluble FP (Siemering, Golbik, Sever, & Haseloff, 1996). Following proper folding, the rate-limiting step for functional chromophore formation is the oxidation of the Tyr66 side chain that brings the aromatic ring of Tyr66 into conjugation with the imidazolone ring. Because this oxidation can take as long as 2 h, there may be a significant lag between GFP translation in cells and GFP fluorescence. The excitation spectrum of *Aequorea* GFP exhibits two absorbance peaks, one at 395 nm and another

at 475 nm, that are thought to result from the protonation state of the chromophore. Protonation of the tyrosine hydroxyl group results in absorbance at 395 nm, and deprotonation to the anionic form of the chromophore yields the 475-nm peak.

5.3 THE STRUCTURE OF GFP

The crystal structure of GFP revealed the importance of the entire GFP protein to the fluorescence of the chromophore. GFP is formed by an 11-stranded β-barrel that folds into a structure that has been termed as β-can (Fig. 5.3; Ormo et al., 1996; Yang, Moss, & Phillips, 1996). The chromophore is completely buried in the center of the β-can structure, protected from solvent quenching effects. Folding of the GFP protein into the β-can structure prevents access of other proteins to the chromophore region; thus, a nonenzymatic mechanism is required for spontaneous chromophore formation. The β-can structure also explains why attempts to truncate GFP to a lower molecular weight were unsuccessful. Almost the entire GFP sequence participates in forming the β-can structure; therefore, the deletion of any part of the sequence would disrupt the overall conformation.

Since the discovery of *Aequorea* GFP, several other FPs from various organisms have been discovered and characterized. Despite their very different sources, all FPs appear to be about 25 kDa and contain similar β-can structures that are necessary for creating the unique environment in which the functional chromophore is formed. So far, only four residues are totally conserved in naturally occurring FPs: Tyr66, Gly67,

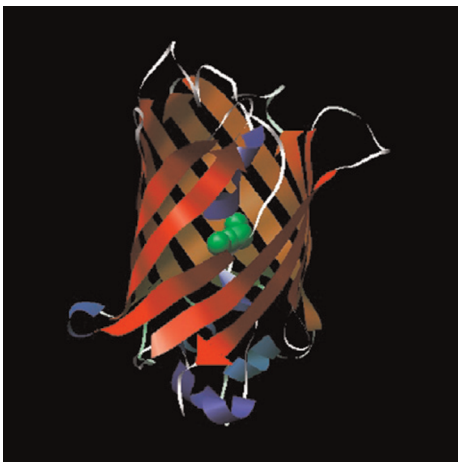

FIGURE 5.3

The structure of GFP. GFP folds into a barrel-like structure composed of 11 strands of β-sheet (shown in red). Buried in the center of the barrel is the GFP chromophore (shown in green).

Arg96, and Tyr222 (Remington, 2006). These residues are necessary for proper chromophore formation and maturation, although studies have shown that other aromatic residues can replace Tyr66 (Heim et al., 1994). Most residues of FPs are not highly conserved, which has allowed for extensive mutagenesis of FPs to optimize and alter their characteristics.

5.4 MUTAGENESIS TO ALTER THE PROPERTIES OF GFP

The thermosensitivity, slow maturation rate, and complex absorbance spectrum of *Aequorea* GFP were some of the factors that prompted multiple research groups to begin mutagenizing GFP to alter its functional properties. Initial mutagenesis studies on GFP were directed at improving its folding and expression at 37 °C and at altering its excitation and emission spectrum (Cormack, Valdivia, & Falkow, 1996; Crameri, Whitehorn, Tate, & Stemmer, 1996; Delagrave, Hawtin, Silva, Yang, & Youvan, 1995; Heim, Cubitt, & Tsien, 1995; Heim et al., 1994; Siemering et al., 1996). These and subsequent studies were quite successful in generating GFP variants that matured rapidly to fluorescence and that absorbed and emitted light at different wavelengths. Excellent reviews of GFP mutagenesis have recently been published that describe a wide variety of mutations and their consequences for GFP fluorescence (Chudakov, Matz, Lukyanov, & Lukyanov, 2010; Day & Davidson, 2009; Kremers, Gilbert, Cranfill, Davidson, & Piston, 2011; Lippincott-Schwartz, & Patterson, 2003; Rizzo, Davidson & Piston, 2009; Shaner, Steinbach, & Tsien, 2005; Zacharias & Tsien, 2006). Furthermore, many other mutations in GFP were generated that favorably altered its properties by reducing its tendency to aggregate, dimerize, or tetramerize, reducing its pH and halide ion sensitivity, and improving its photobleach characteristics.

A major barrier to expanding the applications of GFP was that, despite extensive mutagenesis, no research group had been able to extend its emission spectrum beyond approximately 530 nm so that GFP variants were not available that emitted longer wavelength red light. The solution to this problem came from the isolation of an FP from a coral species *Discosoma* that naturally exhibited a red fluorescence (Matz et al., 1999). This protein, termed drFP583 or dsRed, exhibited an emission peak at 583 nm. The chromophore of dsRed is formed by cyclization of the peptide backbone at amino acids Gln66-Tyr67-Gly68 in a manner analogous to GFP chromophore formation. The extended wavelength fluorescence is due in large part to an additional oxidation of the peptide backbone at Gln66 that extends the conjugated system of the chromophore (Fig. 5.4; Gross, Baird, Hoffman, Baldridge, & Tsien, 2000; Wall, Socolich, & Ranganathan, 2000). However, dsRed exhibits an extremely slow maturation time (>10 h) proceeding through a green intermediate and is an obligate tetramer (Baird, Zacharias & Tsien, 2000).

The discovery of a red fluorescent protein (RFP) provided the platform for further mutagenesis to optimize dsRed for use in cell biology. Bevis & Glick, 2002 first addressed the slow maturation time of dsRed and generated mutants that matured 15 times faster than the original dsRed protein, as well as mutants that reduced

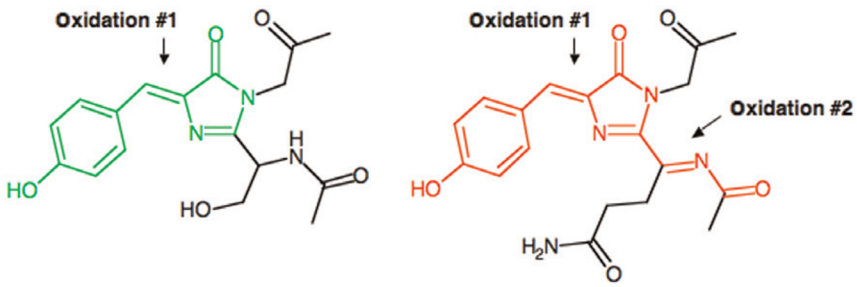

FIGURE 5.4

Comparison of the GFP and dsRed chromophores. The GFP chromophore is shown in green on the left. dsRed (right) contains an additional double bond that extends the conjugated system of the chromophore.

the green intermediate. Through an extensive series of mutagenesis and optimization experiments, Campbell et al., 2002 systematically disrupted the dimer–dimer interface and then the dimer–monomer interface of dsRed to generate a truly monomeric RFP called mRFP1. This monomeric RFP then served as the starting point to diversify the wavelength distribution of RFPs. Continued mutagenesis and optimization allowed Roger Tsien's laboratory to produce an extraordinary array of monomeric RFP derivatives that span the emission spectrum from 537 to 649 nm (Shaner et al., 2004; Wang, Jackson, Steinbach, & Tsien, 2004). Recent advances in expanding the FP color palette include the development of FP variants with improved brightness and photostability, and variants that extend the FP spectrum into the violet and far-red regions (Davidson & Campbell, 2009; Day & Davidson, 2009; Kremers et al., 2011; Rizzo et al., 2009b; Shaner et al., 2008; Shaner, Patterson, & Davidson, 2007; Shcherbo et al., 2009). Development and optimization of more FPs that excite in the far-red end of the spectrum will not only extend the possible number of colors but also most likely improve many aspects of imaging, as longer excitation wavelengths can penetrate deeper into biological tissues, causing less background autofluorescence and less phototoxicity. Table 5.1 lists current GFP variants, grouped by wavelength, that are recommended for conventional imaging applications. This represents a small subset of the diversity of FPs that are available and others that are not listed may be more suitable for specialized applications.

A major advance in FPs was the development of photoactivatable FPs. Patterson & Lippincott-Schwartz, 2002 developed a variant of *Aequorea* GFP by directed mutagenesis called photoactivatable GFP, or PA-GFP, that exhibited very low fluorescence when irradiated with 488-nm light but when activated by irradiation with 413-nm light became 100-fold more fluorescent upon 488 nm excitation. This ability to switch an FP from an "off" state to an "on" state made it possible to spatially activate a subpopulation of the FP within a cell to follow its dynamics through time and space. In the same year, Ando, Hama, Yamamoto-Hino, Mizuno, & Miyawaki, 2002 described an FP from a stony coral that normally exhibits green fluorescence

Table 5.1 Characteristics of selected fluorescent proteins

Fluorescent protein	Ex	Em	ε	QY	Brightness
Violet					
Sirius	355	424	15,000	0.24	3600
Blue					
EBFP2	383	448	32,000	0.56	17,920
Azurite	384	450	26,200	0.55	14,410
mTagBFP	399	456	52,000	0.63	32,760
Cyan					
mTurquoise	434	474	30,000	0.84	25,200
ECFP	434	476	32,500	0.40	13,000
Cerulean	433	475	43,000	0.62	26,660
CyPet	435	477	35,000	0.51	17,850
mTFP1	462	492	64,000	0.85	54,400
Green					
EGFP	488	507	56,000	0.60	33,600
Emerald	487	509	57,500	0.68	39,100
mWasabi	493	509	70,000	0.80	56,000
T-Sapphire	399	511	44,000	0.60	26,400
Yellow					
EYFP	514	527	83,400	0.61	50,874
Venus	515	528	92,200	0.57	52,554
Citrine	516	529	77,000	0.76	58,520
YPet	517	530	104,000	0.77	80,080
Orange					
Kusabira Orange2	551	565	63,800	0.62	39,556
mOrange2	549	565	58,000	0.60	34,800
tdTomato	554	581	138,000	0.69	95,220
TagRFP	555	584	100,000	0.48	48,000
Red					
mApple	568	592	75,000	0.49	36,750
mStrawberry	574	596	90,000	0.29	26,100
mCherry	587	610	72,000	0.22	15,840
Far-red					
mKate2	588	633	62,500	0.40	25,000
mPlum	590	649	41,000	0.10	4100

Ex, excitation maximum (nm); Em, emission maximum (nm); ε, extinction coefficient (M^{-1} cm^{-1}); QY, quantum yield; Brightness, $\varepsilon \times QY$ (M^{-1} cm^{-1}). For a comprehensive analysis of fluorescent protein properties, we recommend these reviews: Chudakov et al. (2010); Davidson and Campbell (2009); Day and Davidson (2009); Kremers et al. (2011); Rizzo et al. (2009a, 2009b); Shaner et al. (2007); Wiedenmann, Oswald, and Nienhaus (2009).
Adapted from Chudakov et al. (2010), Kremers et al. (2011), and Rizzo et al. (2009b) and values in the literature.

but can be switched to red fluorescence by activation with UV light. These initial observations then led to the discovery of several new FPs that can be photoactivated or photoconverted to a new wavelength (Chudakov et al., 2003, 2004; Gurskaya et al., 2006; Tsutsui, Karasawa, Shimizu, Nukina & Miyawaki, 2005; Wiedenmann et al., 2004). Ando, Mizuno, & Miyawaki, 2004 described a novel FP from the coral *Pectiniidae* that could be photoactivated with 400-nm light to become fluorescent-like PA-GFP, but could then be reversibly switched off by irradiation with 490-nm light. This process of "reversible protein highlighting" with reversibly switchable FPs, or RSFPs, allows exquisite spatial control of FP activation in cells. Recent years have seen continued development and optimization of photoactivatable, photoconvertible, and photoswitchable FPs, as they are extremely useful in selectively marking subcellular regions to understand protein dynamics within living systems, as well as in achieving subdiffraction-resolution images of labeled cellular structures when combined with super-resolution imaging techniques (Fig. 5.5; Gould, Verkhusha, & Hess, 2009; Hofmann, Eggeling, Jakobs, & Hell, 2005; Hoi et al., 2010; Lippincott-Schwartz & Patterson, 2009; Lukyanov, Chudakov, Lukyanov, & Verkhusha, 2005; Patterson, Davidson, Manley, & Lippincott-Schwartz, 2010; Wiedenmann et al., 2011; Wiedenmann & Nienhaus, 2006).

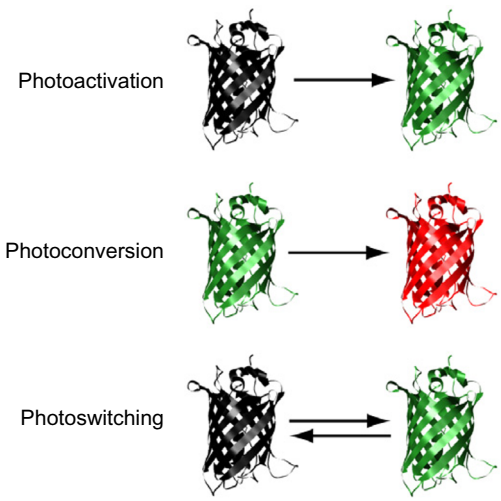

FIGURE 5.5

Switching states in fluorescent proteins. Photoactivation (top) is the process of changing a fluorescent protein from a dark state to a fluorescent state. Photoconversion (middle) involves switching a fluorescent protein from one wavelength emission to a new wavelength emission. Photoswitching (bottom) is the reversible activation and inactivation of a fluorescent protein either from a dark to a fluorescent state or between different wavelengths.

5.5 IMAGING FPs

There are several simple factors to consider and control when planning an imaging experiment that will dramatically improve the ability to detect FPs in fixed or live specimens. Most of these factors are just as applicable to imaging conventional fluorophores as they are to FPs and thus can be considered as general guidelines for fluorescence imaging. The challenge with any live cell experiment is to image the specimen over a long enough time frame to extract meaningful data. This is almost always practically limited by bleaching of the fluorophore and the death of the specimen. These two limitations are often linked through radical generation during photobleaching that causes cellular damage leading to cell death.

5.5.1 Components of the optical system

Designing an optical system to most effectively detect fluorescent signal while minimizing phototoxicity is the first important step in FP imaging. The efficiency of the optical system to detect the fluorescence signal depends on the numerical aperture of the lens, the quality of transmission of the light through the system, and the sensitivity of the detector. High numerical aperture objective lenses allow the collection of more of the fluorescence emission into the optical system and provide more photons for detection. Thus, the highest numerical aperture objective that is available in an appropriate magnification should be selected. Unnecessary optical elements in an imaging system can absorb significant amounts of light. Controlling the light path so that emitted light takes the most direct path to the detector through the least number of optical elements will ensure maximum transmission of signal through the optical system. Finally, once the light reaches the detector, it is important to maximize the detector sensitivity so that as many incident photons as possible are acquired. CCD cameras vary significantly in their spectral response and sensitivity, thus choosing a camera that has high quantum efficiency and sensitivity in the visible wavelengths is recommended.

5.5.2 Reducing unwanted fluorescence

Fluorescence from sources other than the FP of interest can obscure the relevant fluorescence signal. Some of the most common sources of unwanted fluorescence are additives of the imaging medium. Cultured cell media often contain pH indicators such as phenol red or serum components that are fluorescent, and yeast and bacterial rich media also contain significant sources of unwanted fluorescence. Because the sample is bathed in the imaging medium, even dimly fluorescent components in the medium can obscure the detection of the desired fluorescence signal. It is often not possible to exclude all components that contribute to media fluorescence; however, using media that lack additives such as phenol red or defined media that do not contain fluorescent components can eliminate a significant source of unwanted fluorescence.

A second major source of unwanted fluorescence is autofluorescence of the sample itself. There are many examples of cellular compartments and tissues that have an intrinsic fluorescence, such as yolk platelets in embryos, chloroplasts in plants, and vacuolar compartments in fungi to name a few. These sources of intrinsic fluorescence are usually not possible to remove; however, they can often be excluded by the appropriate choice of optical filters.

5.5.3 Selecting appropriate filters and chromatic mirrors

One of the most important factors in maximizing fluorescent signal detection while minimizing unwanted fluorescence signal is the proper matching of the excitation and emission wavelengths of the optical system to the excitation and emission spectrum of the FP. Many imaging systems come equipped with standard filters for DNA dyes such as DAPI or Hoechst, and common fluorophores such as fluorescein or rhodamine. Laser-based systems depend on the emission spectrum of the laser for the excitation wavelength and select emission wavelengths using a variety of methods, ranging from standard emission filters to diffraction-based wavelength selection. However, commonly used wavelengths may not be well suited to the spectrum of a particular FP, and improper matching of the excitation and emission wavelengths will result in significant loss of fluorescence emission signal as well as excessive irradiation of the specimen. The spectrum of EGFP is reasonably well matched to conventional fluorescein excitation and emission filters, and EGFP is efficiently excited by the strong 488-nm emission of the Argon laser. Other FPs, however, require excitation and emission filters that are appropriately matched to their spectra. The yellow fluorescent protein (YFP) variants listed in Table 5.1 are an excellent example. These variants are bright and photostable, but if conventional filter sets are used, the vast majority of the excitation and emission light will be wasted while unnecessarily irradiating the sample. Figure 5.6 shows the difference in image intensity when GFP is imaged through a well-matched filter set versus a poorly matched set.

5.5.4 Selecting the appropriate FP

Although a large number of FPs are currently available, selecting an FP for a specific experiment can be simplified with a few straightforward considerations. The most important consideration in choosing an FP is to maximize its brightness and stability. The data in Table 5.1 can be used to determine the relative brightness of a particular FP in comparison with others. Brightness is calculated by multiplying the extinction coefficient, a measure of how efficiently an FP absorbs light, and the quantum yield, the fraction of absorbed photons that are emitted as fluorescence. For instance, the cyan fluorescent protein (CFP) variant Cerulean is more than twice as bright as ECFP and thus would likely perform better in a standard imaging experiment. Several other factors will also contribute to the apparent brightness of an FP in cells. The expression of the protein can have a major effect on the FP signal. Most available FP variants have been codon optimized for efficient expression in mammalian cells;

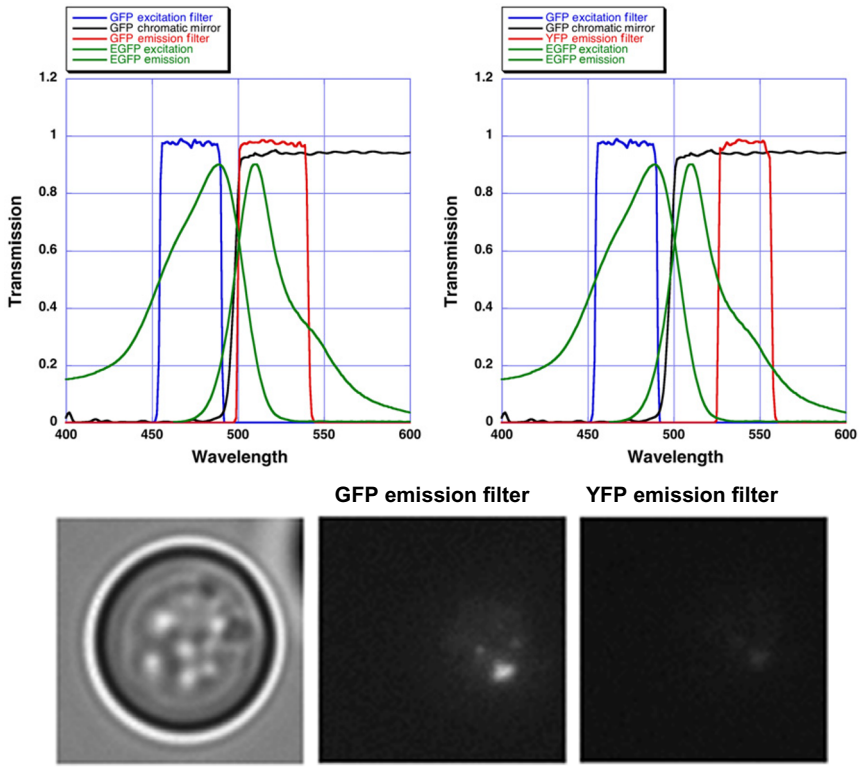

FIGURE 5.6

Choosing the appropriate filter sets for fluorescent protein imaging. Top left panel: excitation and emission spectrum of EGFP (green) and transmission profile of excitation filter (blue), chromatic mirror (black), and emission filter (red) designed for GFP. The top right panel shows the same curves except the emission filter is designed for YFP (red). Bottom panel: brightfield image of yeast cell (left), fluorescence image of yeast cell acquired using GFP filter (center), and fluorescence image of yeast cell acquired using the YFP emission filter.

however, these constructs may be suboptimal when introduced into another organism. We recommend altering the codon bias of the FP so that it matches the most frequently used codons in a particular organism. As previously mentioned, FP folding and maturation rate can have a dramatic effect on apparent fluorescence in cells. Furthermore, wild type GFP is both halide and pH sensitive, a significant consideration if an FP must function in acidic cellular compartments such as the lysosome. Many of the most commonly used FPs have been engineered to fold efficiently at 37 °C, to mature rapidly, and to fluoresce at a wide range of pH and salt concentrations, but being aware of their limitations will help one to circumvent easily avoidable pitfalls.

Several additional factors can affect the ability to image FPs in living cells. FPs exhibit distinctly different quantum photobleach rates, and these rates will determine the duration of imaging experiments (Shaner et al., 2004). Although it is difficult to compare data from many sources on photobleach rates for different FP variants, selecting FPs that have slow bleaching rates can significantly improve the duration and reliability of an imaging experiment. Finally, protein multimerization provides a major obstacle to the use of some FP variants. As mentioned earlier, dsRed is an obligate tetramer when expressed (Baird et al., 2000). Thus, the fusion of a protein of interest to dsRed will naturally tetramerize the protein of interest, leading to unpredictable and likely unwanted effects. Two solutions to this multimerization problem have been devised. The first was to encode a multimer as a fusion in a single repeated reading frame so that a tandem dimer was produced (Campbell et al., 2002). Although this solves the multimerization problem, it also more than doubles the size of the FP and may have deleterious results. An alternative strategy is to use the available monomeric versions of FPs that have very low intermolecular affinities. This will ensure that artifacts of dimerization or multimerization do not adversely affect the imaging experiment. For a more comprehensive analysis and recommendations on FP choice, we recommend the following reviews (Chudakov et al., 2010; Day & Davidson, 2009; Kremers et al., 2011; Lippincott-Schwartz & Patterson, 2003; Rizzo, Davidson, & Piston, 2009a; Rizzo et al., 2009b; Shaner et al., 2005; Wiedenmann et al., 2009; Zacharias & Tsien, 2006).

5.5.5 Constructing FP fusions

One of the most widely used applications of FPs is the fluorescent tagging of another protein of interest in order to follow its localization and dynamics in living systems. However, proteins tagged with FPs may not always recapitulate the behavior of the endogenous protein (Landgraf, Okumus, Chien, Baker, & Paulsson, 2012). In order to have the highest confidence that the behavior of the FP fusion accurately reflects the behavior of the endogenous protein, three criteria should be met. First, one should determine whether fusing an FP to a protein of interest alters the localization of the fusion with respect to the endogenous protein. If an antibody is available to the protein of interest, the localization of the endogenous protein can be determined and compared with that of the FP fusion. In the absence of an antibody, it is often useful to compare N- and C-terminal fusion of proteins to FPs to determine if they report the same localization. Because GFP is 27 kDa, it is also often useful to compare the localization of the FP fusion with the localization of a fusion protein with an alternative antigen tag of smaller size. Second, the construction of an FP should not alter the activity of the protein of interest. If the protein of interest can be produced *in vitro* and has an enzymatic activity, then the FP fusion can easily be tested in the same assay to determine whether the fusion protein changes the activity or kinetics of the enzyme. In practice, it can be difficult to monitor the activity of the protein if its function is unknown or if it is difficult to express or purify. Third, the FP fusion should not alter the stability or expression of the protein of interest. This can often be determined if an antibody to the protein of interest is available. By comparing the

levels of the fusion protein with the levels of the endogenous protein, one can determine whether the FP fusion is produced at a level comparable to the endogenous protein or whether the half-life of the protein changes when fused to the FP. Although satisfying all of these criteria is often not feasible, addressing as many as possible will help one to ensure that the data acquired with the FP fusion accurately reports the behavior of the cellular protein.

5.5.6 Note on fixation of FPs

The advantage of FP imaging comes as a result of detecting the protein in living cells, but there are many instances where fixation of the cells and imaging of the FP are desirable. Fixation of FP fusions can give highly variable results. Excessive fixation or the use of harsh fixatives can destroy the fluorescence of GFP. As a general rule, short fixation with paraformaldehyde or formaldehyde often preserves the fluorescence of GFP as well as maintains the localization of the protein of interest, whereas soluble GFP has been shown to be extracted by methanol fixation (Wang, Miller, Shaw, & Shaw, 1996). As a cautionary note, the spectral properties of CFP have been reported to change significantly after aldehyde fixation, although this does not seem to be a general property of FPs (Domin Lan, & Kaminski, 2004). A careful analysis of FP redistribution was performed under different fixation conditions to monitor the localization of the epidermal growth factor receptor (EGFR; Brock, Hamelers, & Jovin, 1999). These authors observed that methanol fixation completely removed EGFR from cells while paraformaldehyde preserved the localization and fluorescence of the fusion protein. These authors also noted that the use of the Mowiol mounting media caused redistribution of the GFP signal in cells. Properties of the mounting media such as pH and halide concentration should be checked for compatibility with the FP used in the experiment. Thus, careful attention should be paid to the fixation and mounting conditions used when analyzing FP distribution in fixed specimens.

5.5.7 Time-lapse imaging of FPs

FP imaging in live cells allows one to study the dynamics of proteins over time and under different stimuli (Fig. 5.7). In order to image labeled cells over long time periods without undue damage to the specimen, it is necessary to optimize the cell growth conditions on the microscope as well as limit the amount of excitation light to which cells are exposed. Many different methods for stage incubation have been developed from simple chambers that hold the specimen on the microscope stage to enclosures for the entire imaging platform that regulate temperature, gas, and humidity. Depending on the sample, finding an appropriate specimen incubator that preserves viability will allow long-term imaging of cells. Finally, limiting the exposure time and intensity of the excitation light will have a substantial effect on sample viability. Most current platforms for time-lapse microscopy include electronic shutters that gate the excitation light and use neutral density filters or electronic modulation to alter the intensity of the excitation beam. Either reducing the time of

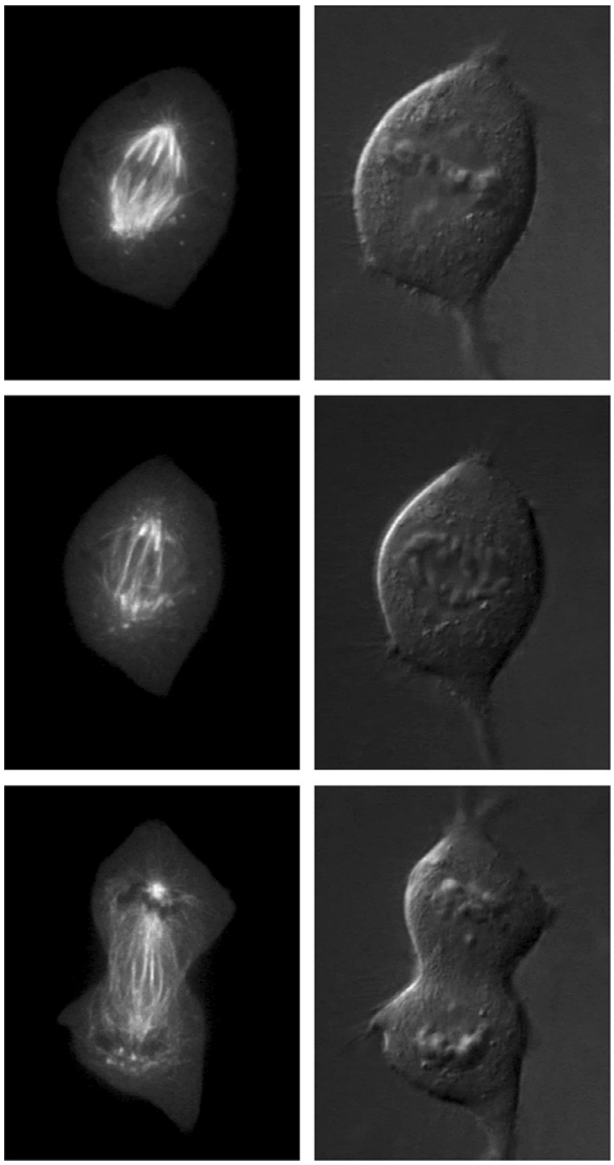

FIGURE 5.7

Example of time-lapse image sequence. Mammalian tissue culture cells growing at 37 °C and expressing a fusion of EGFP to α-tubulin were imaged through the process of mitosis using fluorescence (left panels) and differential interference contrast microscopy (right panels). Top panel, metaphase; center panel, early anaphase; and bottom panel, late anaphase.

excitation with high-intensity light or decreasing the intensity of excitation in a given timeframe is an effective means of reducing photodamage, and the choice between these alternatives should be empirically determined as appropriate for the specimen. Reducing photobleaching and photodamage to the specimen and optimizing growth conditions will facilitate effective live cell imaging over longer time periods.

5.6 APPLICATIONS OF FP IMAGING

The development of FP variants that possess diverse properties such as spectral differences, sensitivity to environmental factors, and photoswitchable responses to light has opened many new avenues in live cell imaging. Here, we discuss a few examples of microscopy-based FP applications to investigate cell biological questions.

5.6.1 Multiwavelength imaging of FPs

The development of many different spectral variants of FPs has enabled the simultaneous imaging of multiple tagged proteins in living cells. There are several combinations of FPs that are well separated in their fluorescence excitation and emission spectra so that they can be easily distinguished with appropriate filter sets. One of the most commonly used pair of FPs for multiple labeling are the cyan and YFPs. Their widespread use primarily reflects the timing of their development, because the longer wavelength dsRed variants were not available until more recently. The bright CFP variants such as Cerulean and CyPet can be easily combined with the YFP variants such as Citrine, YPet, and Venus for simultaneous imaging. The development of longer wavelength FPs has enabled dual wavelength imaging of GFP variants and Red variants such as mStrawberry, mCherry, and mPlum. It is now common practice to distinguish three and four FP variants simultaneously within a single cell, given the appropriate selection of excitation and emission filters (Shaner et al., 2005). With the continued development of spectral unmixing technologies, one may be able to distinguish several FPs within a single cell.

5.6.2 Monitoring intracellular environments using FPs

The sensitivity of some FP variants to factors such as pH and halide ion concentration served as a starting point to generate reporters of cellular environment. One of the first examples of this was to exploit the changes in excitation and emission spectra of FPs in response to pH changes to obtain a readout of the pH of different cellular compartments (Llopis, McCaffery, Miyawaki, Farquhar, & Tsien, 1998; Miesenbock, De Angelis, & Rothman, 1998). In an elegant study describing pH-dependent indicators called pHluorins, Miesenbock and Rothman demonstrated that the ratio of emission intensity of pHluorins when excited at 410 and 470 nm depended upon the pH of the environment. Using the ratio of emission intensities at different excitation wavelengths, they were able to accurately calculate the pH of different compartments of the secretory pathway.

The discovery of spectral variants of GFP made possible the use of Förster resonance energy transfer (FRET) to generate sensors of intracellular environment and enzyme activity. Two fluorescent molecules such as CFP and YFP have excitation and emission spectra such that there is significant overlap of the CFP emission spectrum with the excitation spectrum of YFP. When brought in close proximity ($<$100 Å), excitation of CFP can result in the radiationless transfer of the excited state energy to YFP, resulting in fluorescence emission at longer wavelengths as YFP returns to the ground state. This FRET process is extremely sensitive to distance, as the efficiency of the energy transfer process drops proportional to the sixth power of the distance between the FP molecules. Miyawaki et al., 1997 used this distance dependence to create intracellular sensors for calcium ion concentration. By inserting the calmodulin protein and a calmodulin-binding peptide between either BFP and GFP or CFP and YFP, the authors were able to generate a sensor that would bring the two FPs into close proximity, and thus increase the energy transfer efficiency, as a function of calcium binding. A number of different biosensors based upon this energy transfer system have now been used to detect cyclic-AMP, sugars, protease activity, kinase activity, and more (Fig. 5.8; Blakeley, Chapman, & McNaughton, 2012; Fehr et al., 2005; Frommer, Davidson, & Campbell, 2009; Honda et al., 2001; Luo, Yu, Pu, & Chang, 2001; Sato, Hida, Ozawa, & Umezawa, 2000; Zaccolo et al., 2000).

5.6.3 Monitoring protein–protein interactions in vivo

The application of FP-based reporters of proximity can also be applied to study the interaction between proteins within living cells. By fusing two different FPs that can act as an energy transfer pair to two different proteins of interest, it is possible to monitor the spatial and temporal interactions between those proteins in cells by monitoring the energy transfer efficiency. This approach was first used to demonstrate that the transcription factor Pit1 could dimerize in the cell nucleus by monitoring the energy transfer efficiency between Pit1 fused to GFP and BFP in the same cell (Periasamy & Day, 1998). Although in principle using energy transfer seems a simple approach to detecting protein–protein interactions in living cells, accurate calculation of energy transfer efficiency can be hampered by many factors. A discussion of the microscopic methods for calculating transfer efficiency between FPs is beyond the scope of this chapter, but these techniques have been extensively reviewed elsewhere (Day & Davidson, 2009; Miyawaki & Tsien, 2000; Piston & Kremers, 2007; Sekar & Periasamy, 2003; Vogel, Thaler, & Koushik, 2006).

Split-FP systems have also proven to be useful as alternatives to FRET-based methods for detecting protein–protein interactions in living cells (Chun, Waldo, & Johnson, 2010; Kerppola, 2008; Shekhawat & Ghosh, 2011). Putative interacting proteins are fused to two nonfluorescing fragments of a split-FP, and when interacting proteins come into close proximity and bind, they reconstitute the intact FP as well as FP fluorescence. This system avoids some of the issues that arise in FRET-based assays, such as low signal and the need to overexpress protein above endogenous levels, but may introduce unique disadvantages, such as slow FP reassembly and susceptibility to aggregation.

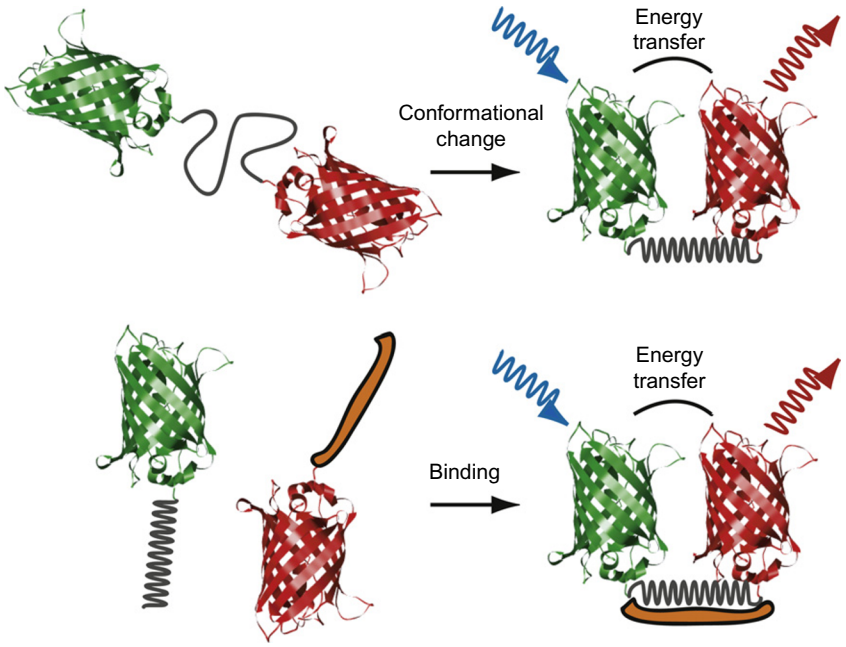

FIGURE 5.8

Using energy transfer between fluorescent proteins to monitor cellular environment and protein interactions. Top panel: a linker between two fluorescent proteins whose conformation changes upon protein or small molecule binding brings two fluorescent proteins into close proximity so that FRET occurs and can be measured to determine the concentration or activity of the linker binding moiety. Bottom panel: two proteins or protein domains that bind to one another when fused to fluorescent proteins can bring the fluorescent proteins into close proximity and thus generate a readout for the interaction of the two proteins within the cell.

5.6.4 Protein dynamic measurements using FP photobleaching and activation

The dynamic properties of proteins in cells can be effectively studied using spatially localized photobleaching and photoactivation of FPs. The best known of these techniques is fluorescence recovery after photobleaching (FRAP), where a defined region of fluorescence signal is ablated using high-intensity light and then the recovery of fluorescence is monitored over time (Axelrod, Koppel, Schlessinger, Elson, & Webb, 1976). This allows an estimate of the mobility of protein within the photobleached region as well as an estimate of how completely fluorescence can be recovered. A companion technique to FRAP is fluorescence loss in photobleaching (FLIP). FLIP employs continuous ablation of the fluorescence in a region of the cell until all cellular fluorescence signal is gone or no more decay due to the bleaching light is observed (Lippincott-Schwartz & Patterson, 2003). This provides an estimate of the total mobility of fluorescent signal within a cell. Finally, the

discovery of FP photoactivation and photoconversion allows a region of the cell to be activated to the fluorescent state and then the relocalization of the fluorescent molecules can be monitored over time as they redistribute (Patterson & Lippincott-Schwartz, 2002). These three techniques allow calculation of protein mobility throughout cells, in specific regions or organelles, and even allow estimates of bulk association, dissociation, and diffusion kinetics in living specimens.

5.6.5 Super-resolution imaging with photoactivatable FPs

The development of photoactivable FPs has led to a revolution in super-resolution imaging. Conventional imaging is limited by the diffraction of light, so that the highest possible resolution is about half the wavelength of the light used, or at least 200 nm. However, many cellular structures and processes are on the level of tens of nanometers, and cannot be resolved by conventional imaging. After the development of the first photoactivable FP, Betzig et al. described a technique called photoactivated localization microscopy, or PALM, which uses low-level illumination to photoactivate a small percentage of PA-FP molecules in a sample (Betzig et al., 2006). The spots corresponding to individual fluorescent PA-FP molecules are still diffraction limited; however, they are sparse enough that they do not overlap, and therefore the center of each spot can be precisely calculated using the point spread function of the microscope. These molecules are then photobleached, and low-level illumination of the sample is repeated to photoactivate new subsets of molecules, eventually resulting in a complete, super-resolution image. PALM, as well as fluorescent photactivation localization microscopy and stochastic optical reconstruction microscopy developed around the same time, are imaging techniques that take advantage of the unique properties of photoactivatable and photoswitchable molecules to achieve subdiffraction resolution (Hess, Girirajan, & Mason, 2006; Rust, Bates, & Zhuang, 2006). These techniques continue to develop and expand to different imaging realms such as multicolor imaging, 3D imaging, and live cell imaging (Chang et al., 2012; Gould et al., 2009; Gunewardene et al., 2011; Huang, Babcock, & Zhuang, 2010; Lippincott-Schwartz & Patterson, 2009; Patterson et al., 2010; Schermelleh, Heintzmann, & Leonhardt, 2010).

CONCLUSION

The examples described earlier represent just a few of the many applications of FP imaging used to understand the dynamics of proteins in cells and to monitor the intercellular environment. Additional applications whose descriptions are outside the scope of this chapter include FP-based sensors of cell cycle state (Sakaue-Sawano et al., 2008), optical control of protein activity (Zhou, Chung, Lam & Lin, 2012), all-optical writing with a photoswitchable GFP (Grotjohann et al., 2011), and many more. As more FP variants are discovered in nature and as more derivatives of FPs are developed in the laboratory, the scope of FP applications will continue to expand. A great deal of work has been done to generate FP wavelength variants with improved brightness and photostability, and new variants continue to be developed

at a rapid rate. Our ability to examine the behavior of proteins within living cells and cells within living organisms has been transformed by the discovery of GFP and will continue to improve with the further development of novel FP applications.

References

Ando, R., Hama, H., Yamamoto-Hino, M., Mizuno, H., & Miyawaki, A. (2002). An optical marker based on the UV-induced green-to-red photoconversion of a fluorescent protein. *Proceedings of the National Academy of Sciences of the United States of America*, *99*(20), 12651–12656.

Ando, R., Mizuno, H., & Miyawaki, A. (2004). Regulated fast nucleocytoplasmic shuttling observed by reversible protein highlighting. *Science*, *306*(5700), 1370–1373.

Axelrod, D., Koppel, D. E., Schlessinger, J., Elson, E., & Webb, W. W. (1976). Mobility measurement by analysis of fluorescence photobleaching recovery kinetics. *Biophysical Journal*, *16*(9), 1055–1069.

Baird, G. S., Zacharias, D. A., & Tsien, R. Y. (2000). Biochemistry, mutagenesis, and oligomerization of DsRed, a red fluorescent protein from coral. *Proceedings of the National Academy of Sciences of the United States of America*, *97*(22), 11984–11989.

Betzig, E., Patterson, G. H., Sougrat, R., Lindwasser, O. W., Olenych, S., Bonifacino, J. S., et al. (2006). Imaging intracellular fluorescent proteins at nanometer resolution. *Science*, *313*(5793), 1642–1645.

Bevis, B. J., & Glick, B. S. (2002). Rapidly maturing variants of the Discosoma red fluorescent protein (DsRed). *Nature Biotechnology*, *20*(1), 83–87.

Blakeley, B. D., Chapman, A. M., & McNaughton, B. R. (2012). Split-superpositive GFP reassembly is a fast, efficient, and robust method for detecting protein–protein interactions in vivo. *Molecular BioSystems*, *8*(8), 2036.

Brock, R., Hamelers, I. H., & Jovin, T. M. (1999). Comparison of fixation protocols for adherent cultured cells applied to a GFP fusion protein of the epidermal growth factor receptor. *Cytometry*, *35*(4), 353–362.

Campbell, R. E., Tour, O., Palmer, A. E., Steinbach, P. A., Baird, G. S., Zacharias, D. A., et al. (2002). A monomeric red fluorescent protein. *Proceedings of the National Academy of Sciences of the United States of America*, *99*(12), 7877–7882.

Chalfie, M., Tu, Y., Euskirchen, G., Ward, W. W., & Prasher, D. C. (1994). Green fluorescent protein as a marker for gene expression. *Science*, *263*(5148), 802–805.

Chang, H., Zhang, M., Ji, W., Chen, J., Zhang, Y., Liu, B., et al. (2012). A unique series of reversibly switchable fluorescent proteins with beneficial properties for various applications. *Proceedings of the National Academy of Sciences of the United States of America*, *109*(12), 4455–4460.

Chudakov, D. M., Belousov, V. V., Zaraisky, A. G., Novoselov, V. V., Staroverov, D. B., Zorov, D. B., et al. (2003). Kindling fluorescent proteins for precise in vivo photolabeling. *Nature Biotechnology*, *21*(2), 191–194.

Chudakov, D. M., Matz, M. V., Lukyanov, S., & Lukyanov, K. A. (2010). Fluorescent proteins and their applications in imaging living cells and tissues. *Physiological Reviews*, *90*(3), 1103–1163.

Chudakov, D. M., Verkhusha, V. V., Staroverov, D. B., Souslova, E. A., Lukyanov, S., & Lukyanov, K. A. (2004). Photoswitchable cyan fluorescent protein for protein tracking. *Nature Biotechnology*, *22*(11), 1435–1439.

Chun, W., Waldo, G. S., & Johnson, G. V. W. (2010). Split GFP complementation assay for quantitative measurement of tau aggregation in situ. *Methods in Molecular Biology*, *670*, 109–123 (Chapter 9).

Cody, C. W., Prasher, D. C., Westler, W. M., Prendergast, F. G., & Ward, W. W. (1993). Chemical structure of the hexapeptide chromophore of the Aequorea green-fluorescent protein. *Biochemistry*, *32*(5), 1212–1218.

Cormack, B. P., Valdivia, R. H., & Falkow, S. (1996). FACS-optimized mutants of the green fluorescent protein (GFP). *Gene*, *173*(1 Spec. No.), 33–38.

Crameri, A., Whitehorn, E. A., Tate, E., & Stemmer, W. P. (1996). Improved green fluorescent protein by molecular evolution using DNA shuffling. *Nature Biotechnology*, *14*(3), 315–319.

Davidson, M. W., & Campbell, R. E. (2009). Engineered fluorescent proteins: Innovations and applications. *Nature Methods*, *6*(10), 713–717.

Day, R. N., & Davidson, M. W. (2009). The fluorescent protein palette: Tools for cellular imaging. *Chemical Society Reviews*, *38*(10), 2887.

Delagrave, S., Hawtin, R. E., Silva, C. M., Yang, M. M., & Youvan, D. C. (1995). Red-shifted excitation mutants of the green fluorescent protein. *Biotechnology (NY)*, *13*(2), 151–154.

Domin, A., Lan, M. J., & Kaminski, C. (2004). Effects of fixation on cyan fluorescent protein and its fluorescence resonance energy transfer efficiency. Paper presented at the Laser Applications to Chemical and Environmental Analysis.

Fehr, M., Okumoto, S., Deuschle, K., Lager, I., Looger, L. L., Persson, J., et al. (2005). Development and use of fluorescent nanosensors for metabolite imaging in living cells. *Biochemical Society Transactions*, *33*(Pt 1), 287–290.

Frommer, W. B., Davidson, M. W., & Campbell, R. E. (2009). Genetically encoded biosensors based on engineered fluorescent proteins. *Chemical Society Reviews*, *38*(10), 2833.

Gould, T. J., Verkhusha, V. V., & Hess, S. T. (2009). Imaging biological structures with fluorescence photoactivation localization microscopy. *Nature Protocols*, *4*(3), 291–308.

Gross, L. A., Baird, G. S., Hoffman, R. C., Baldridge, K. K., & Tsien, R. Y. (2000). The structure of the chromophore within DsRed, a red fluorescent protein from coral. *Proceedings of the National Academy of Sciences of the United States of America*, *97*(22), 11990–11995.

Grotjohann, T., Testa, I., Leutenegger, M., Bock, H., Urban, N. T., Lavoie-Cardinal, F., et al. (2011). Diffraction-unlimited all-optical imaging and writing with a photochromic GFP. *Nature*, 1–5.

Gunewardene, M. S., Subach, F. V., Gould, T. J., Penoncello, G. P., Gudheti, M. V., Verkhusha, V. V., et al. (2011). Superresolution imaging of multiple fluorescent proteins with highly overlapping emission spectra in living cells. *Biophysical Journal*, *101*(6), 1522–1528.

Gurskaya, N. G., Verkhusha, V. V., Shcheglov, A. S., Staroverov, D. B., Chepurnykh, T. V., Fradkov, A. F., et al. (2006). Engineering of a monomeric green-to-red photoactivatable fluorescent protein induced by blue light. *Nature Biotechnology*, *24*(4), 461–465.

Hastings, J. W., & Morin, J. G. (1969). Comparative biochemistry of calcium-activated photoproteins from the Ctenophore, Mnemiopsis and the coelenterates Aequorea, Obelia, Pelagia and Renilla. *The Biological Bulletin*, *137*, 402.

Heim, R., Cubitt, A. B., & Tsien, R. Y. (1995). Improved green fluorescence. *Nature*, *373*(6516), 663–664.

Heim, R., Prasher, D. C., & Tsien, R. Y. (1994). Wavelength mutations and posttranslational autoxidation of green fluorescent protein. *Proceedings of the National Academy of Sciences of the United States of America*, *91*(26), 12501–12504.

Hess, S. T., Girirajan, T. P. K., & Mason, M. D. (2006). Ultra-high resolution imaging by fluorescence photoactivation localization microscopy. *Biophysical Journal*, *91*(11), 4258–4272.

Hofmann, M., Eggeling, C., Jakobs, S., & Hell, S. W. (2005). Breaking the diffraction barrier in fluorescence microscopy at low light intensities by using reversibly photoswitchable proteins. *Proceedings of the National Academy of Sciences of the United States of America*, *102*(49), 17565–17569.

Hoi, H., Shaner, N. C., Davidson, M. W., Cairo, C. W., Wang, J., & Campbell, R. E. (2010). A monomeric photoconvertible fluorescent protein for imaging of dynamic protein localization. *Journal of Molecular Biology*, *401*(5), 776–791.

Honda, A., Adams, S. R., Sawyer, C. L., Lev-Ram, V., Tsien, R. Y., & Dostmann, W. R. (2001). Spatiotemporal dynamics of guanosine 3′,5′-cyclic monophosphate revealed by a genetically encoded, fluorescent indicator. *Proceedings of the National Academy of Sciences of the United States of America*, *98*(5), 2437–2442.

Huang, B., Babcock, H., & Zhuang, X. (2010). Breaking the diffraction barrier: Super-resolution imaging of cells. *Cell*, *143*(7), 1047–1058.

Inouye, S., & Tsuji, F. I. (1994). Aequorea green fluorescent protein. Expression of the gene and fluorescence characteristics of the recombinant protein. *FEBS Letters*, *341*(2–3), 277–280.

Johnson, F. H., Shimomura, O., Saiga, Y., Gershman, L. C., Reynolds, G. T., & Waters, J. R. (1962). Quantum efficiency of Cypridina luminescence, with a note on that of Aequorea. *Journal of Cellular and Comparative Physiology*, *60*, 85–104.

Kerppola, T. K. (2008). Bimolecular fluorescence complementation (BiFC) analysis as a probe of protein interactions in living cells. *Annual Review of Biophysics*, *37*(1), 465–487.

Kremers, G. J., Gilbert, S. G., Cranfill, P. J., Davidson, M. W., & Piston, D. W. (2011). Fluorescent proteins at a glance. *Journal of Cell Science*, *124*(15), 2676.

Landgraf, D., Okumus, B., Chien, P., Baker, T. A., & Paulsson, J. (2012). Segregation of molecules at cell division reveals native protein localization. *Nature Methods*, *9*(5), 480–482.

Lippincott-Schwartz, J., & Patterson, G. H. (2003). Development and use of fluorescent protein markers in living cells. *Science*, *300*(5616), 87–91.

Lippincott-Schwartz, J., & Patterson, G. H. (2009). Photoactivatable fluorescent proteins for diffraction-limited and super-resolution imaging. *Trends in Cell Biology*, *19*(11), 555–565.

Llopis, J., McCaffery, J. M., Miyawaki, A., Farquhar, M. G., & Tsien, R. Y. (1998). Measurement of cytosolic, mitochondrial, and Golgi pH in single living cells with green fluorescent proteins. *Proceedings of the National Academy of Sciences of the United States of America*, *95*(12), 6803–6808.

Lukyanov, K. A., Chudakov, D. M., Lukyanov, S., & Verkhusha, V. V. (2005). Innovation: Photoactivatable fluorescent proteins. *Nature Reviews. Molecular Cell Biology*, *6*(11), 885–891.

Luo, K. Q., Yu, V. C., Pu, Y., & Chang, D. C. (2001). Application of the fluorescence resonance energy transfer method for studying the dynamics of caspase-3 activation during UV-induced apoptosis in living HeLa cells. *Biochemical and Biophysical Research Communications*, *283*(5), 1054–1060.

Matz, M. V., Fradkov, A. F., Labas, Y. A., Savitsky, A. P., Zaraisky, A. G., Markelov, M. L., et al. (1999). Fluorescent proteins from nonbioluminescent Anthozoa species. *Nature Biotechnology*, *17*(10), 969–973.

Miesenbock, G., De Angelis, D. A., & Rothman, J. E. (1998). Visualizing secretion and synaptic transmission with pH-sensitive green fluorescent proteins. *Nature*, *394*(6689), 192–195.

Miyawaki, A., Llopis, J., Heim, R., McCaffery, J. M., Adams, J. A., Ikura, M., et al. (1997). Fluorescent indicators for Ca^{2+} based on green fluorescent proteins and calmodulin. *Nature*, *388*(6645), 882–887.

Miyawaki, A., & Tsien, R. Y. (2000). Monitoring protein conformations and interactions by fluorescence resonance energy transfer between mutants of green fluorescent protein. *Methods in Enzymology*, *327*, 472–500.

Morin, J. G., & Hastings, J. W. (1971). Energy transfer in a bioluminescent system. *Journal of Cellular Physiology*, *77*(3), 313–318.

Morise, H., Shimomura, O., Johnson, F. H., & Winant, J. (1974). Intermolecular energy transfer in the bioluminescent system of Aequorea. *Biochemistry*, *13*(12), 2656–2662.

Ormo, M., Cubitt, A. B., Kallio, K., Gross, L. A., Tsien, R. Y., & Remington, S. J. (1996). Crystal structure of the *Aequorea victoria* green fluorescent protein. *Science*, *273*(5280), 1392–1395.

Patterson, G., Davidson, M., Manley, S., & Lippincott-Schwartz, J. (2010). Superresolution imaging using single-molecule localization. *Annual Review of Physical Chemistry*, *61*(1), 345–367.

Patterson, G. H., & Lippincott-Schwartz, J. (2002). A photoactivatable GFP for selective photolabeling of proteins and cells. *Science*, *297*(5588), 1873–1877.

Periasamy, A., & Day, R. N. (1998). FRET imaging of Pit-1 protein interactions in living cells. *Journal of Biomedical Optics*, *3*(2), 154–160.

Piston, D. W., & Kremers, G.-J. (2007). Fluorescent protein FRET: The good, the bad and the ugly. *Trends in Biochemical Sciences*, *32*(9), 407–414.

Prasher, D. C., Eckenrode, V. K., Ward, W. W., Prendergast, F. G., & Cormier, M. J. (1992). Primary structure of the *Aequorea victoria* green-fluorescent protein. *Gene*, *111*(2), 229–233.

Reid, B. G., & Flynn, G. C. (1997). Chromophore formation in green fluorescent protein. *Biochemistry*, *36*(22), 6786–6791.

Remington, S. J. (2006). Fluorescent proteins: Maturation, photochemistry and photophysics. *Current Opinion in Structural Biology*, *16*(6), 714–721.

Rizzo, M. A., Davidson, M. W., & Piston, D. W. (2009a). Fluorescent protein tracking and detection: Applications using fluorescent proteins in living cells. *Cold Spring Harbor Protocols*, *2009*(12), pdb.top64.

Rizzo, M. A., Davidson, M. W., & Piston, D. W. (2009b). Fluorescent protein tracking and detection: Fluorescent protein structure and color variants. *Cold Spring Harbor Protocols*, *2009*(12), pdb.top63.

Rust, M. J., Bates, M., & Zhuang, X. (2006). Sub-diffraction-limit imaging by stochastic optical reconstruction microscopy (STORM). *Nature Methods*, *3*(10), 793–796.

Sakaue-Sawano, A., Kurokawa, H., Morimura, T., Hanyu, A., Hama, H., Osawa, H., et al. (2008). Visualizing spatiotemporal dynamics of multicellular cell-cycle progression. *Cell*, *132*(3), 487–498.

Sato, M., Hida, N., Ozawa, T., & Umezawa, Y. (2000). Fluorescent indicators for cyclic GMP based on cyclic GMP-dependent protein kinase Ialpha and green fluorescent proteins. *Analytical Chemistry*, *72*(24), 5918–5924.

Schermelleh, L., Heintzmann, R., & Leonhardt, H. (2010). A guide to super-resolution fluorescence microscopy. *The Journal of Cell Biology*, *190*(2), 165–175.

Sekar, R. B., & Periasamy, A. (2003). Fluorescence resonance energy transfer (FRET) microscopy imaging of live cell protein localizations. *The Journal of Cell Biology*, *160*(5), 629–633.

Shaner, N. C., Campbell, R. E., Steinbach, P. A., Giepmans, B. N., Palmer, A. E., & Tsien, R. Y. (2004). Improved monomeric red, orange and yellow fluorescent proteins

derived from *Discosoma* sp. red fluorescent protein. *Nature Biotechnology*, *22*(12), 1567–1572.

Shaner, N. C., Lin, M. Z., McKeown, M. R., Steinbach, P. A., Hazelwood, K. L., Davidson, M. W., et al. (2008). Improving the photostability of bright monomeric orange and red fluorescent proteins. *Nature Methods*, *5*(6), 545–551.

Shaner, N. C., Patterson, G. H., & Davidson, M. W. (2007). Advances in fluorescent protein technology. *Journal of Cell Science*, *120*(24), 4247–4260.

Shaner, N. C., Steinbach, P. A., & Tsien, R. Y. (2005). A guide to choosing fluorescent proteins. *Nature Methods*, *2*(12), 905–909.

Shcherbo, D., Murphy, C. S., Ermakova, G. V., Solovieva, E. A., Chepurnykh, T. V., Shcheglov, A. S., et al. (2009). Far-red fluorescent tags for protein imaging in living tissues. *The Biochemical Journal*, *418*(3), 567.

Shekhawat, S. S., & Ghosh, I. (2011). Split-protein systems: Beyond binary protein–protein interactions. *Current Opinion in Chemical Biology*, *15*(6), 789–797.

Shimomura, O. (1979). Structure of the chromophore of Aequorea green fluorescent protein. *FEBS Letters*, *104*, 220–222.

Shimomura, O., Johnson, F. H., & Saiga, Y. (1962). Extraction, purification and properties of aequorin, a bioluminescent protein from the luminous hydromedusan, *Aequorea*. *Journal of Cellular and Comparative Physiology*, *59*, 223–239.

Siemering, K. R., Golbik, R., Sever, R., & Haseloff, J. (1996). Mutations that suppress the thermosensitivity of green fluorescent protein. *Current Biology*, *6*(12), 1653–1663.

Tsutsui, H., Karasawa, S., Shimizu, H., Nukina, N., & Miyawaki, A. (2005). Semi-rational engineering of a coral fluorescent protein into an efficient highlighter. *EMBO Reports*, *6*(3), 233–238.

Vogel, S. S., Thaler, C., & Koushik, S. V. (2006). Fanciful FRET. *Science's STKE*, *2006*(331), re2.

Wall, M. A., Socolich, M., & Ranganathan, R. (2000). The structural basis for red fluorescence in the tetrameric GFP homolog DsRed. *Natural Structural Biology*, *7*(12), 1133–1138.

Wang, L., Jackson, W. C., Steinbach, P. A., & Tsien, R. Y. (2004). Evolution of new nonantibody proteins via iterative somatic hypermutation. *Proceedings of the National Academy of Sciences of the United States of America*, *101*(48), 16745–16749.

Wang, D. S., Miller, R., Shaw, R., & Shaw, G. (1996). The pleckstrin homology domain of human beta I sigma II spectrin is targeted to the plasma membrane in vivo. *Biochemical and Biophysical Research Communications*, *225*(2), 420–426.

Wiedenmann, J., Gayda, S., Adam, V., Oswald, F., Nienhaus, K., Bourgeois, D., et al. (2011). From EosFP to mIrisFP: Structure-based development of advanced photoactivatable marker proteins of the GFP-family. *Journal of Biophotonics*, *4*(6), 377–390.

Wiedenmann, J., Ivanchenko, S., Oswald, F., Schmitt, F., Rocker, C., Salih, A., et al. (2004). EosFP, a fluorescent marker protein with UV-inducible green-to-red fluorescence conversion. *Proceedings of the National Academy of Sciences of the United States of America*, *101*(45), 15905–15910.

Wiedenmann, J., & Nienhaus, G. U. (2006). Live-cell imaging with EosFP and other photoactivatable marker proteins of the GFP family. *Expert Review of Proteomics*, *3*(3), 361–374.

Wiedenmann, J., Oswald, F., & Nienhaus, G. U. (2009). Fluorescent proteins for live cell imaging: Opportunities, limitations, and challenges. *IUBMB Life*, *61*(11), 1029–1042.

Yang, F., Moss, L. G., & Phillips, G. N., Jr. (1996). The molecular structure of green fluorescent protein. *Nature Biotechnology*, *14*(10), 1246–1251.

Zaccolo, M., De Giorgi, F., Cho, C. Y., Feng, L., Knapp, T., Negulescu, P. A., et al. (2000). A genetically encoded, fluorescent indicator for cyclic AMP in living cells. *Nature Cell Biology*, *2*(1), 25–29.

Zacharias, D. A., & Tsien, R. Y. (2006). Molecular biology and mutation of green fluorescent protein. *Methods of Biochemical Analysis*, *47*, 83–120.

Zhou, X. X., Chung, H. K., Lam, A. J., & Lin, M. Z. (2012). Optical control of protein activity by fluorescent protein domains. *Science*, *338*(6108), 810–814.